The Canadian Mineralogist
Vol. 37, pp. 99-112 (1999)

Sr-BEARING PEROVSKITE AND LOPARITE FROM LAMPROITE AND AGPAITIC NEPHELINE SYENITE PEGMATITES

ROGER H. MITCHELL[1] AND ANTON R. CHAKHMOURADIAN

Department of Geology, Lakehead University, 955 Oliver Road, Thunder Bay, Ontario P7B 5E1

Abstract

The paragenesis and compositional variation of strontium-bearing perovskite and loparite occurring in lamproites and agpaitic nepheline syenite pegmatites are described. Olivine lamproites from West Kimberley (Australia), Kapamba (Zambia) and Prairie Creek – American Mine (Arkansas) typically contain perovskite with complex oscillatory zoning and a low Sr content (<3 wt.% SrO). Perovskite in olivine-free madupitic lamproite from the Leucite Hills (Wyoming) is enriched in Sr (3–7 wt.% SrO) and rare-earth elements relative to perovskite occurring in olivine lamproite. The perovskite in the lamproite from Hills Pond (Kansas) is unusual in containing Si (0.2–2.0 wt.% SiO_2), being relatively-enriched in Sr (3–6 wt.% SrO), and exhibiting complex sector-zoning. Perovskite crystals from lamproites show no regularities in zonation trends, which may be either of increasing or decreasing Sr content from core to rim. Agpaitic nepheline syenite pegmatites from Pegmatite Peak and Gordon Butte (Montana) contain strontian calcian loparite (10–19 wt.% SrO), and are significantly enriched in Sr relative to loparite found in agpaitic nepheline syenites from the Khibina and Lovozero (Russia) complexes. Naturally occurring perovskite-group minerals exhibit a continuous solid-solution between tausonite and loparite-(Ce), but not between tausonite and perovskite. The Sr-rich perovskite, strontian loparite, and ceroan tausonite are found only in alkaline silicate rocks that lack primary carbonates; Na–Sr-poor, Nb-rich perovskite belonging to the perovskite – latrappite – lueshite series form in SiO_2-poor environments characterized by the presence of primary carbonate. In the magmas that form the latter rocks, Sr is preferentially partitioned into carbonates rather than titanates.

Keywords: perovskite, loparite, tausonite, lamproite, agpaitic nepheline syenite, carbonatite.

Sommaire

Nous décrivons la paragenèse et les variations en composition de la pérovskite et la loparite strontifère que nous trouvons dans les lamproïtes et les syénites néphéliniques à tendance agpaïtique et à caractère pegmatitique. Les lamproïtes à olivine de West Kimberley (Australie), Kapamba (Zambie) et Prairie Creek – American Mine (Arkansas) contiennent typiquement une pérovskite ayant une zonation complexe oscillatoire et une faible teneur en Sr (<3% SrO, poids). La pérovskite des lamproïtes madupitiques sans olivine provenant de Leucite Hills (Wyoming) est enrichie en Sr (3–7 wt.% SrO) et les terres rares par rapport à la pérovskite des lamproïtes à olivine. La pérovskite de la lamproïte de Hills Pond (Kansas) est atypique en contenant Si (0.2–2.0 wt.% SiO_2), en étant relativement enrichie en Sr (3–6% SrO, poids), et en possédant une zonation en secteurs complexe. Les cristaux de pérovskite provenant des lamproïtes n'ont pas de régularité dans leur zonation en Sr, qui peut donc aller en augmentant ou en diminuant du centre d'un grain vers la bordure. Les syénites néphéliniques agpaïtiques pegmatitiques de Pegmatite Peak et Gordon Butte (Montana) contiennent une loparite strontifère et calcique (10–19% SrO, poids); elle est définitivement enrichie en Sr par rapport à la loparite des syénites néphéliniques agpaïtiques des massifs de Khibina et de Lovozero (Russie). Les exemples naturels font partie d'une solution solide continue entre tausonite et loparite-(Ce), mais non entre tausonite et pérovskite. On trouve la pérovskite riche en Sr, la loparite strontifère et la tausonite enrichie en cérium seulement dans les roches alcalines silicatées sans carbonates primaires; la pérovskite à faible teneur en Na et Sr, et enrichie en Nb, faisant partie de la série pérovskite – latrappite – lueshite, cristallise dans des milieux à faible teneur en silice, et en présence de carbonate primaire. Dans les systèmes magmatiques qui ont donné de telles roches, le Sr serait préférentiellement réparti dans les carbonates plutôt que les titanates.

(Traduit par la Rédaction)

Mots-clés: pérovskite, loparite, tausonite, lamproïte, syénite néphélinique agpaïtique, carbonatite.

[1] *E-mail address*: rmitchel@gale.lakeheadu.ca

Introduction

Perovskite-group minerals that contain more than 1 wt.% SrO are relatively uncommon compared to Sr-poor, Nb-rich perovskite that is ubiquitous in many alkaline undersaturated rocks such as kimberlite, melilitite and carbonatite. Currently, little is known of their paragenesis and compositional variation. Previous studies have focussed on Sr-rich perovskite from potassium-rich silicate rocks such as lamproite (Mitchell 1995a, Mitchell & Steele 1992), orangeite (Mitchell 1995a), ultrapotassic syenite (Mitchell & Vladykin 1993) and rheomorphic fenite (Haggerty & Mariano 1983). In these studies, summarized by Mitchell (1996), the authors have demonstrated that most of the compositional variation may be described in terms of solid solution between the end-member components: $CaTiO_3$ (perovskite), $SrTiO_3$ (tausonite), $NaNbO_3$ (lueshite), and $Na(REE)Ti_2O_6$ (loparite). The Sr-rich perovskite-group mineral tausonite is known only from the Little Murun ultrapotassic complex (Vorobyev *et al.* 1984).

The previous studies, with the exception of that of Mitchell & Vladykin (1993), were of a reconnaissance nature. The objective of the present work is to document in detail the paragenesis and compositional variation shown by Sr-bearing perovskite in lamproites and diverse agpaitic nepheline syenite pegmatites. These data fill a lacuna in our knowledge of the overall compositional variation exhibited by perovskite in alkaline rocks, and are a prerequisite for an understanding of why Sr-rich perovskite appears to form only in alkaline silicate rocks.

Analytical Techniques

All mineral compositions were determined by X-ray energy-dispersion spectrometry (EDS) using a Hitachi 570 scanning electron microscope equipped with a LINK ISIS analytical system incorporating a Super ATW Light Element Detector (133 eV FwHm Mn*K*) at Lakehead University. EDS spectra were acquired for 180 or 300 seconds (live time) with an accelerating voltage of 20 kV and beam current of 0.86 nA. X-ray spectra were collected and processed with the LINK ISIS – SEMQUANT software package. Full ZAF corrections were applied to the raw X-ray data. The following well-characterized standards were employed for the determination of mineral compositions: Khibina loparite (Na, La, Ce, Pr, Nd, Nb,), Magnet Cove perovskite (Ti, Ca, Fe), synthetic $SrTiO_3$ (Sr), and metallic Th and Ta. A multi-element standard for the rare-earth elements (*REE*) was used as, in our experience, it gives more accurate data than single-*REE* standards when using EDS spectrum-stripping techniques. However, peak profiles used for the analytical X-ray lines were obtained using single *REE* fluoride standards. The accuracy of the method was cross-checked by wavelength-dispersion electron-microprobe analysis of some samples using an automated CAMECA SX–50 microprobe located at the University of Manitoba using methods described by Mitchell & Vladykin (1993). Ba was not detected in any of the samples analyzed, even though these commonly coexist with Ba-rich minerals.

The back-scattered electron (BSE) images were acquired with the LINK ISIS – AUTOBEAM function using a Hitachi 570 scanning electron microscope. The images were given false colors using the LINK ISIS – SPEEDMAP software package and stored as digital ".pcx" files. The false colors are defined by the relative contrast and brightness of the BSE images and reflect the average atomic number of individual phases. We consider that false-color images of this type are superior to conventional half-tone BSE-images in illustrating the subtleties of zoning and minor compositional variation.

Mitchell (1996) has demonstrated that the compositions of most naturally occurring perovskite-group minerals can be expressed in terms of relatively few end-member compositions, namely: $CaTiO_3$ (perovskite), $Na(REE)Ti_2O_6$ (loparite), $NaNbO_3$ (lueshite), and $SrTiO_3$ (tausonite), with lesser amounts of $Ca_2Fe^{3+}NbO_6$ (latrappite), $Ca_2Nb_2O_7$, $REE_2Ti_2O_7$, $CaThO_3$, $CaZrO_3$, $KNbO_3$, $PbTiO_3$ (macedonite) and $BaTiO_3$. Compositional data were recalculated into these perovskite-group end-member compounds using an APL program for PC following methods suggested by Mitchell (1996).

Perovskite in Lamproite: Compositional Variation

Perovskite-group minerals are relatively rare in the majority of lamproites, the principal hosts for titanium being priderite and jeppeite (Mitchell & Bergman 1991). Perovskite *sensu stricto,* together with Cr-rich spinel, occurs only in olivine and madupitic lamproites; these rocks commonly lack other titanates.

Olivine lamproites are typically hypabyssal holocrystalline rocks consisting principally of forsterite-rich olivine phenocrysts and xenocrysts, together with diopside and phlogopite. Olivine lamproites are currently considered to be hybrid rocks whose bulk compositions are in part determined by contamination with mantle-derived ultrabasic material. Their petrological status remains controversial. Mitchell & Bergman (1991), Mitchell (1995b) and Edgar & Mitchell (1997) do not regard olivine lamproites as being parental to the relatively more common silica-rich phlogopite or leucite lamproites. In contrast, Jaques *et al.* (1986) regarded olivine lamproites as relatively unevolved members of the lamproite clan. Discussion of this controversy is beyond the scope of this work. Summaries may be found in Mitchell (1995b) and Mitchell & Bergman (1991). Many occurrences of olivine lamproite are associated with diamond deposits, although they themselves typically are very poor or lacking in diamond. Also included in this survey are examples of madupitic lamproites,

which may or may not contain olivine; they are characterized by the presence of poikilitic phlogopite in the groundmass.

West Kimberley, Australia

In the olivine lamproites of the West Kimberley province (Jaques *et al.* 1986), groundmass perovskite occurs as minute (6–50 μm, average 20–25 μm across) subhedral crystals that commonly contain ovoid inclusions of olivine or apatite. Associated groundmass minerals include phlogopite, apatite, titanian potassium richterite, wadeite, priderite and altered sanidine. The crystals typically show complex zonation, which may be of the following varieties: (1) an oscillatory type without changes in overall habit from core to rim, with up to 20 thin (<5 μm) zones per crystal (Figs. 1a, b, c, 2a, b), (2) an oscillatory type with a core differing in morphology from the overgrowth (Figs. 1a, c, 2, a, c, d), and (3) a sectorally zoned type (Fig. 2e).

Table 1 and Figure 3 demonstrate that perovskite from West Kimberley has a restricted range in composition, low contents of Nb, Na and Th, and that the rare-earth elements and Sr are the significant minor elements. Recalculation of the compositions into end-member perovskite components (Table 1) demonstrates that the minerals principally represent solid solutions involving the end members perovskite, loparite and tausonite. In most cases, the perovskite contains greater than 90 mol.% $CaTiO_3$ and is thus classified as perovskite *sensu stricto* (Table 1, Fig. 3). Cores of crystals containing up to 12.1 wt.% $LREE_2O_3$ (>10 mol.% $NaCeTi_2O_6$) may be termed ceroan perovskite (Fig. 3). Although Sr-bearing, none of the perovskite analyzed is sufficiently rich in Sr to be termed strontian perovskite or tausonite.

The striking oscillatory zonation evident in the BSE-images primarily reflects differences of only 1–2 wt.% total *REE* between zones (Fig. 3). Individual zones thus exhibit a trend of increased or decreased content of

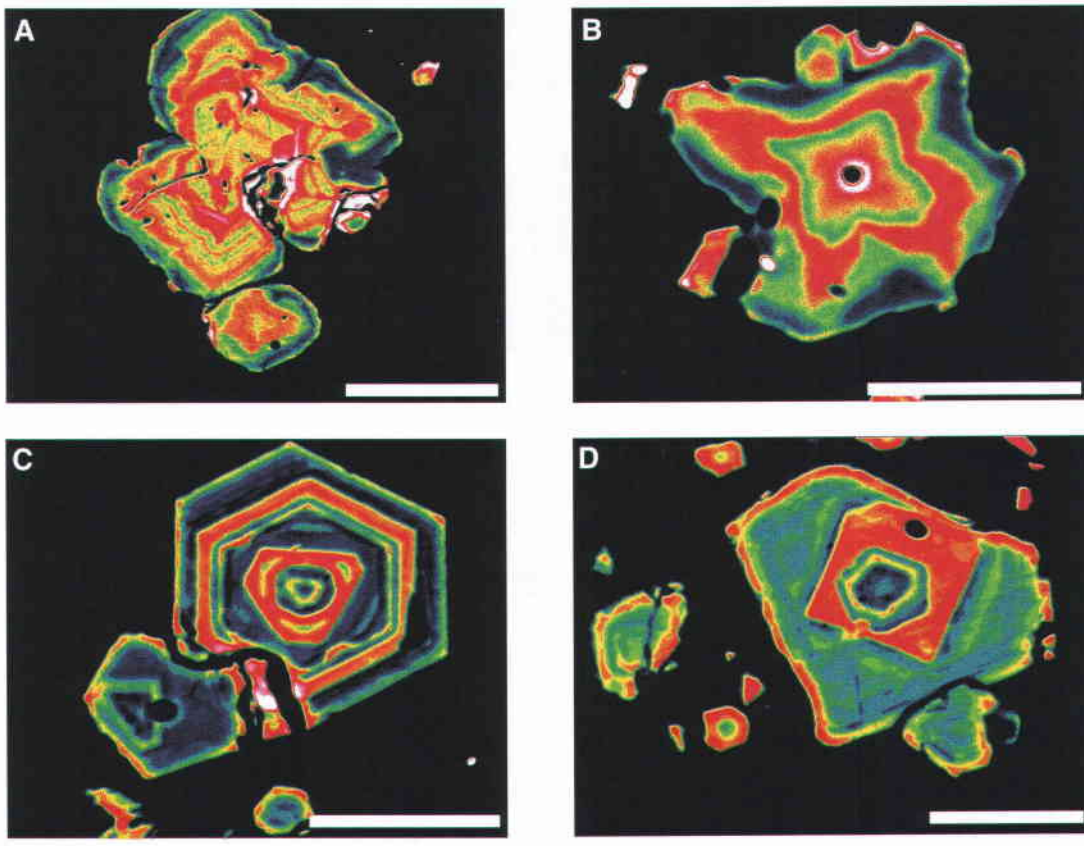

FIG. 1. Styles of oscillatory zoning in perovskite from olivine lamproites (A–B, Ellendale 11, D–C, Ellendale 4) from West Kimberley, Australia. A–C type 1, D type 2 (see text). False-color back-scattered electron image.

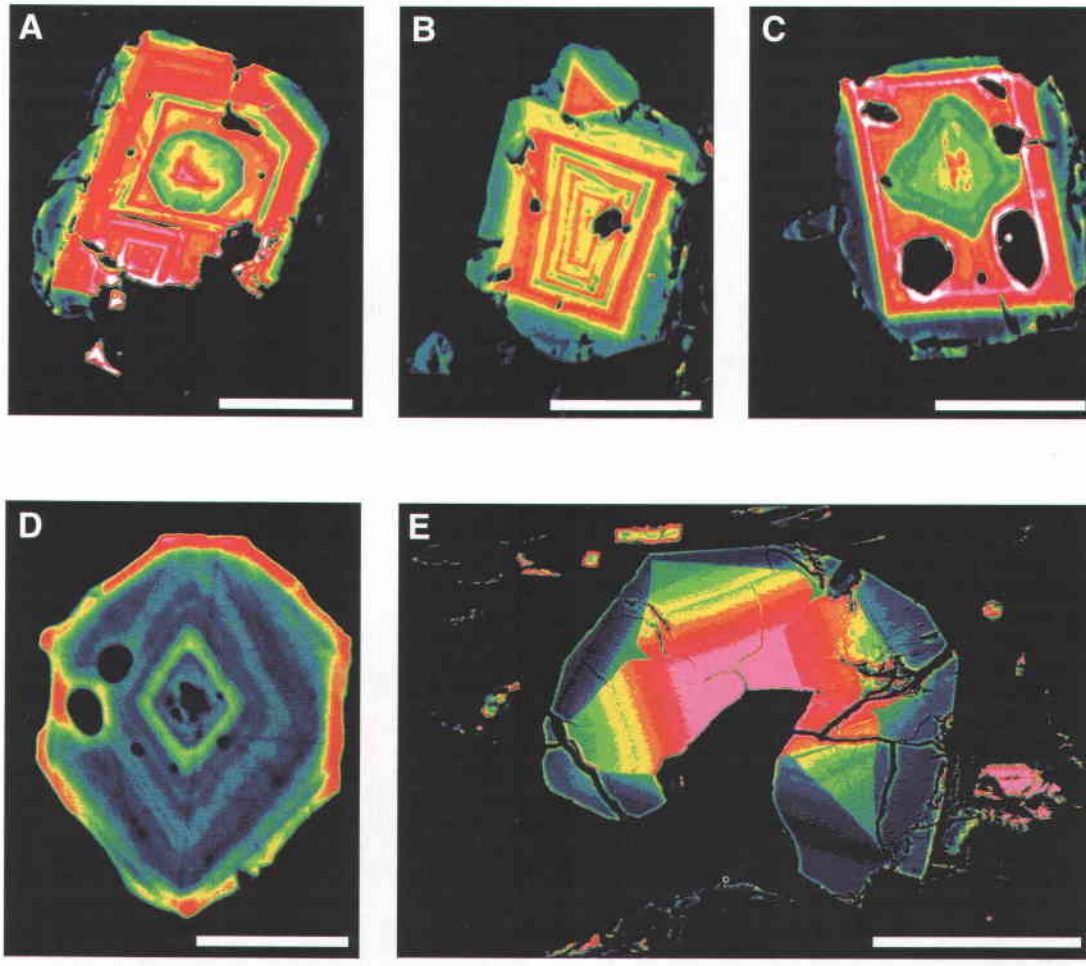

FIG. 2. Styles of oscillatory zoning in perovskite from olivine lamproite from: West Kimberley (A–C, Ellendale 9), American mine; Arkansas (D), Hills Pond, Kansas (E). A–D type 2, E type 3 (see text). False-color back-scattered electron image.

loparite relative to each other, upon which is superimposed an overall trend of depletion in the loparite component (11 → 4 mol.%) from core to rim. Sector-zoned crystals are characterized by growth sectors that are relatively enriched or depleted by about 1–3 wt.% total *REE*. Crystals of complex morphology (Fig. 1a) reflect similar compositional variations.

The following overall core-to-rim patterns of zonation were observed: (a) decreasing loparite content combined with increasing tausonite (1–2 mol.%) content (Fig. 3b), and (b) decreasing loparite content at essentially constant tausonite content (Figs. 3a, c, d).

Perovskite is also known from pegmatitic rocks of the Walgidee Hills, where it occurs as complexly twinned, pale green to brownish yellow, weakly oscillatory zoned subhedral crystals. The perovskite coexists with priderite, jeppeite, shcherbakovite, wadeite and titanian potassium richterite. These minerals are set in a turbid matrix considered to be altered K-feldspar. The perovskite is compositionally similar to that found in the olivine lamproites (Mitchell & Reed 1988, Mason 1977).

Prairie Creek, Arkansas

In olivine lamproite from Prairie Creek, perovskite forms subhedral to euhedral crystals averaging 20–25 μm in size in the groundmass. Rarely, grains up to 60 μm are found. The crystals typically enclose tiny silicate inclusions that are too small to analyze. Associated minerals include diopside, chromian spinel, apatite and poikilitic phlogopite in the groundmass.

Complex oscillatory zonation similar to that observed in West Kimberley perovskite is commonly

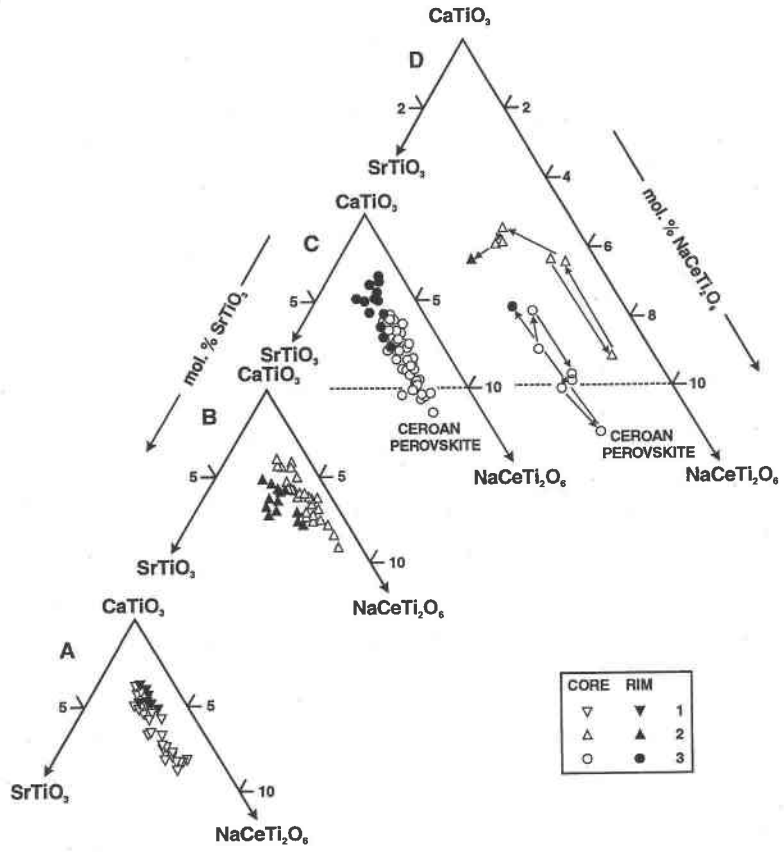

FIG. 3. Compositional variation (mol.%) of perovskite from West Kimberley olivine lamproite. (A) Ellendale 4, (B) Ellendale 11, (C) Ellendale 9, (D) typical patterns of zonation.

present. Many of the zones are irregular in morphology, suggesting that repeated episodes of dissolution and growth occurred.

Representative compositions given in Table 2 indicate that the perovskite is extremely poor in minor elements and is essentially $CaTiO_3$ (>95 mol.%), with small amounts of solid solution toward loparite (0.5–8 mol.%) and tausonite (0.5–4 mol.%). Figure 4 illustrates that the compositional zoning reflects small changes in total *REE* contents coupled with an overall trend of loparite depletion and tausonite enrichment from core to rim. The zonation trend is similar to the trend of Sr-enrichment found in some of the West Kimberley perovskite.

American Mine, Arkansas

Perovskite in olivine lamproite from the American Mine occurs as minute (up to 20 μm) crystals with very poorly developed or no oscillatory zonation. Two-phase mantled crystals occur rarely. Representative compositions given in Table 2 indicate that this perovskite is identical to that occurring in the nearby Prairie Creek olivine lamproite. Patterns of zonation, where present, also are similar (Fig. 5). The overall trend of compositional evolution shows no Sr enrichment and culminates with almost pure $CaTiO_3$ perovskite (Fig. 5).

Kapamba, Zambia

In the Kapamba olivine madupitic lamproites (Scott Smith *et al.* 1989), perovskite crystals range in habit from euhedral discrete crystals in the groundmass (intrusions P1/5 and P2/12) to anhedral oikocrysts (intrusion P6/8), ranging from 20 to 40 μm across. The discrete crystals may enclose tiny crystals of Cr–Mg–Al-bearing spinel. The oikocrysts fill the interstices between phlogopite plates, apatite and clinopyroxene, in some cases enclosing these minerals. BSE-imagery reveals no obvious compositional zonation.

TABLE 1. COMPOSITIONS OF PEROVSKITE FROM OLIVINE LAMPROITES

Wt.%	1	2	3	4	5	6	7	8	9	10
Nb_2O_5	0.23	0.59	0.60	0.49	0.78	0.40	0.79	0.99	0.36	0.52
Ta_2O_5	0.39	0.39	0.44	0.90	0.89	0.73	0.43	0.36	0.34	0.56
TiO_2	52.52	56.49	54.01	56.55	54.53	54.78	52.86	56.31	54.42	57.19
Fe_2O_3	1.11	0.83	1.60	1.19	1.86	1.45	1.35	0.69	1.26	1.05
ThO_2	0.10	0.01	0.25	n.d	n.d	n.d	0.44	n.d	0.18	n.d
La_2O_3	2.89	1.15	n.d	n.d	0.39	0.20	2.44	0.55	1.20	n.d
Ce_2O_3	6.36	1.60	4.29	1.72	1.62	2.42	3.78	0.74	4.37	1.33
Pr_2O_3	1.19	n.d	n.d	n.d	n.d	n.d	0.12	n.d	n.d	n.d
Nd_2O_3	1.65	0.07	n.d	n.d	n.d	0.11	1.06	n.d	1.21	n.d
CaO	31.38	36.26	35.27	38.89	36.26	36.60	33.89	36.43	34.47	38.10
SrO	1.70	2.01	1.43	1.22	1.29	1.06	0.71	2.01	1.54	1.32
Na_2O	0.78	0.77	0.69	0.45	0.79	0.71	0.83	0.99	0.64	0.77
Total	100.29	100.17	98.58	101.41	98.40	98.46	98.70	99.07	99.99	100.84
Structural formulae based on 3 atoms of oxygen										
Nb	0.002	0.006	0.006	0.005	0.008	0.004	0.009	0.010	0.004	0.005
Ta	0.003	0.002	0.003	0.006	0.006	0.005	0.003	0.002	0.002	0.003
Ti	0.965	0.987	0.969	0.972	0.968	0.973	0.962	0.987	0.973	0.983
Fe	0.020	0.014	0.029	0.021	0.033	0.026	0.025	0.012	0.022	0.018
Th	0.001	0.000	0.001	0.000	0.000	0.000	0.002	0.000	0.001	0.000
La	0.026	0.010	0.000	0.000	0.003	0.002	0.022	0.005	0.011	0.000
Ce	0.057	0.014	0.038	0.014	0.014	0.021	0.033	0.006	0.038	0.011
Pr	0.011	0.000	0.000	0.000	0.000	0.000	0.001	0.000	0.000	0.000
Nd	0.014	0.001	0.000	0.000	0.000	0.001	0.009	0.000	0.010	0.000
Ca	0.821	0.902	0.901	0.952	0.917	0.926	0.879	0.910	0.878	0.933
Sr	0.024	0.027	0.020	0.016	0.018	0.015	0.010	0.027	0.021	0.017
Na	0.037	0.035	0.032	0.020	0.036	0.033	0.039	0.045	0.029	0.034
Mol.% End-members										
$CaThO_3$	0.06	0.00	0.14	0.00	0.00	0.00	0.25	0.00	0.10	0.00
$SrTiO_3$	2.62	2.74	2.01	1.62	1.78	1.46	1.03	2.74	2.21	1.76
$NaNbO_3$	0.00	1.08	0.00	0.56	1.90	0.90	0.00	3.40	0.00	2.31
$CaTiO_3$	89.28	91.31	91.37	94.94	92.80	92.91	90.66	91.64	91.53	93.70
Loparite	8.04	4.87	6.48	2.88	3.52	4.73	8.06	2.22	6.16	2.23

Compositions 1-10 West Kimberley, Australia: 1 & 2 # 77439 (Ellendale 2), 3 & 4 # 71469H (Ellendale 4), 5 & 6 # 71461 (Ellendale 9), 7 & 8 # 71453M (Ellendale 11), 9 & 10 71478H (Ellendale 4). Total Fe expressed as Fe_2O_3; n.d = not detected.

Representative data given in Table 3 show that perovskite from Kapamba exhibits a wider range in composition than perovskite from other olivine lamproites, ranging from perovskite *sensu stricto* (discrete phases in the groundmass) to ceroan strontian perovskite (oikocrysts). The latter are enriched in Sr (up to 5.1 wt.% SrO), the light rare-earth elements (*LREE*, up to 6.7 wt.% $LREE_2O_3$), Na (up to 2.5 wt.% Na_2O), and Nb (up to 1.9 wt.% Nb_2O_5). Individual intrusions appear, on the basis of the data given in Figure 6, to contain perovskite of distinct compositions. Although zoning is absent, the overall evolutionary trend, interpreted from petrographic data, is one of increasing Sr and *REE* content.

Hills Pond, Kansas

Perovskite occurs rarely in the Hills Pond olivine richterite diopside lamproite sills (Cullers *et al.* 1985, Mitchell & Bergman 1991). The perovskite forms anhedral grains up to 200 μm in size, filling in the interstices between the silicates, suggesting that it is a late-stage groundmass mineral. Rarely, a Ba–K titanosilicate is found along fractures in perovskite. This silicate $[(Ba_{0.41}K_{0.31}Na_{0.26}Ca_{0.19})_{\Sigma 1.17}(Ti_{0.96}Mg_{0.11}Fe_{0.03}Nb_{0.02})$

TABLE 2. REPRESENTATIVE COMPOSITIONS OF PEROVSKITE FROM OLIVINE LAMPROITES

Wt.%	1	2	3	4	5	6	7	8	9	10	11	12
Nb_2O_5	0.43	0.51	0.27	0.34	0.27	0.41	0.28	0.55	0.12	0.40	0.41	0.24
Ta_2O_5	0.14	0.63	0.26	0.57	0.12	0.55	0.21	0.65	0.29	0.27	0.48	0.76
TiO_2	55.02	57.43	54.40	58.17	55.22	57.38	54.94	58.06	56.09	56.87	56.75	53.78
Fe_2O_3	1.48	0.31	1.78	0.59	1.29	0.37	1.27	0.19	1.44	1.24	1.22	1.24
ThO_2	n.d	n.d	n.d	n.d	n.d	n.d	n.d	n.d	0.05	n.d	n.d	n.d
La_2O_3	2.10	0.13	1.66	0.37	1.99	0.80	2.21	n.d	1.83	0.27	0.92	1.62
Ce_2O_3	2.61	0.42	2.73	0.72	1.94	0.32	3.14	0.20	3.18	0.65	2.25	2.60
Pr_2O_3	n.d	0.28	n.d	n.d	n.d	n.d	n.d	n.d	n.d	n.d	n.d	n.d
Nd_2O_3	0.25	0.29	0.51	n.d	n.d	n.d	n.d	n.d	n.d	0.14	n.d	0.41
CaO	37.18	36.99	36.89	37.38	37.42	37.17	37.06	37.78	37.15	38.24	38.08	35.95
SrO	0.53	2.19	1.05	2.83	0.64	2.33	0.87	2.57	0.51	0.65	0.69	0.62
Na_2O	0.39	1.08	0.36	0.81	0.25	1.09	0.28	1.01	0.45	0.39	0.57	0.81
Total	100.13	100.26	99.91	101.78	99.14	100.42	100.26	101.01	101.11	99.12	101.37	98.03
Structural formulae based on 3 atoms of oxygen												
Nb	0.005	0.005	0.003	0.003	0.003	0.004	0.003	0.006	0.001	0.004	0.004	0.003
Ta	0.001	0.004	0.002	0.003	0.001	0.003	0.001	0.004	0.002	0.002	0.003	0.005
Ti	0.968	0.994	0.963	0.994	0.975	0.992	0.969	0.995	0.976	0.988	0.977	0.969
Fe	0.026	0.005	0.032	0.010	0.023	0.006	0.022	0.003	0.025	0.022	0.021	0.022
Th	0.000	0.000	0.000	0.000	0.000	0.000	0.000	0.000	0.000	0.000	0.000	0.000
La	0.018	0.001	0.014	0.003	0.017	0.008	0.019	0.000	0.016	0.002	0.008	0.014
Ce	0.022	0.004	0.024	0.006	0.017	0.002	0.027	0.002	0.027	0.005	0.019	0.023
Pr	0.000	0.002	0.000	0.000	0.000	0.000	0.000	0.000	0.000	0.000	0.000	0.000
Nd	0.002	0.002	0.004	0.000	0.000	0.000	0.000	0.000	0.000	0.001	0.000	0.003
Ca	0.932	0.913	0.930	0.910	0.941	0.915	0.931	0.922	0.921	0.946	0.934	0.923
Sr	0.007	0.029	0.014	0.037	0.009	0.031	0.012	0.034	0.007	0.009	0.009	0.009
Na	0.018	0.048	0.017	0.036	0.011	0.049	0.013	0.045	0.020	0.017	0.025	0.038
Mol.% End-members												
$CaThO_3$	0.00	0.00	0.00	0.00	0.00	0.00	0.00	0.00	0.03	0.00	0.00	0.00
$SrTiO_3$	0.74	2.93	1.47	3.76	0.90	3.09	1.22	3.39	0.71	0.89	0.92	0.87
$NaNbO_3$	0.00	3.89	0.00	2.68	0.00	3.89	0.00	4.28	0.00	0.87	0.00	0.00
$CaTiO_3$	95.63	91.31	95.17	91.73	96.77	91.13	96.15	92.00	95.09	96.42	93.99	91.54
Loparite	3.63	1.87	3.36	1.83	2.33	1.89	2.63	0.33	4.17	1.82	5.09	7.59

Compositions 1-8 Prairie Creek, Arkansas: 1 & 2 ARK-1, 3 & 4 ARK-2, 5 & 6 ARK-3, 7 & 8 ARK-5; 9-12 American Mine, Arkansas: 9 & 10 AKM-2, 11 AKM-3, 12 AKM-4. Total Fe expressed as Fe_2O_3; n.d = not detected.

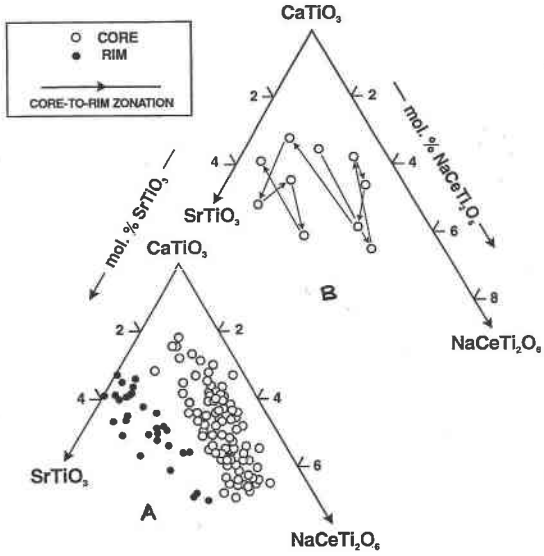

FIG. 4. Compositional variation (mol.%) of perovskite from the Prairie Creek olivine lamproite. (A) Overall compositional range of cores and rims of discrete crystals; (B) typical core-to-rim patterns of zonation.

TABLE 3. REPRESENTATIVE COMPOSITIONS OF PEROVSKITE AND LOPARITE FROM OLIVINE LAMPROITES

Wt.%	1	2	3	4	5	6	7	8	9	10
Nb_2O_5	0.73	0.75	0.70	0.71	0.73	0.72	1.81	0.40	0.92	1.57
Ta_2O_5	0.47	0.44	0.47	0.47	0.64	0.33	0.57	n.d	n.d	n.d
TiO_2	55.91	55.82	53.70	54.86	57.35	55.68	55.01	46.95	50.55	54.50
SiO_2	n.d	n.d	n.d	n.d	n.d	n.d	n.d	0.55	1.07	0.19
Fe_2O_3	2.22	1.81	2.18	2.62	0.95	0.70	0.69	0.45	0.33	0.29
ThO_2	n.d	n.d	0.88	n.d	n.d	0.13	0.23	0.77	0.38	0.13
La_2O_3	0.10	0.92	0.23	0.97	0.51	1.12	1.03	7.49	3.96	1.26
Ce_2O_3	1.18	2.38	1.60	2.89	1.45	2.66	3.40	15.76	9.04	3.74
Pr_2O_3	n.d	n.d	n.d	n.d	0.19	0.58	0.24	1.15	0.99	0.90
Nd_2O_3	0.46	0.17	0.83	0.40	0.44	0.58	0.99	3.39	3.43	1.98
CaO	39.20	38.94	38.05	38.07	35.49	34.28	30.36	12.26	20.93	30.05
SrO	0.31	0.23	0.32	0.43	1.52	1.97	4.79	5.69	4.87	3.65
Na_2O	0.23	0.22	0.24	0.55	1.37	1.33	2.49	3.83	3.13	2.08
K_2O	n.d	n.d	n.d	n.d	n.d	n.d	n.d	1.23	0.89	0.21
Total	100.81	101.68	99.20	101.97	100.74	100.08	101.61	99.92	100.49	100.55
Structural formulae based on 3 atoms of oxygen										
Nb	0.008	0.008	0.007	0.007	0.008	0.008	0.019	0.005	0.011	0.017
Ta	0.003	0.003	0.003	0.003	0.004	0.002	0.004	0.000	0.000	0.000
Ti	0.962	0.960	0.951	0.948	0.993	0.985	0.978	0.970	0.965	0.981
Si	0.000	0.000	0.000	0.000	0.000	0.000	0.000	0.015	0.027	0.004
Fe	0.038	0.031	0.039	0.045	0.016	0.012	0.012	0.009	0.006	0.005
Th	0.000	0.000	0.005	0.000	0.000	0.001	0.001	0.005	0.002	0.001
La	0.001	0.008	0.002	0.008	0.004	0.010	0.009	0.076	0.037	0.011
Ce	0.010	0.020	0.014	0.024	0.012	0.023	0.029	0.159	0.084	0.033
Pr	0.000	0.000	0.000	0.000	0.002	0.005	0.002	0.011	0.009	0.008
Nd	0.004	0.001	0.007	0.003	0.004	0.005	0.008	0.033	0.031	0.017
Ca	0.962	0.955	0.960	0.938	0.875	0.864	0.769	0.361	0.569	0.771
Sr	0.004	0.003	0.004	0.006	0.020	0.027	0.066	0.091	0.072	0.051
Na	0.010	0.010	0.011	0.025	0.061	0.061	0.114	0.204	0.154	0.097
K	0.000	0.000	0.000	0.000	0.000	0.000	0.000	0.043	0.029	0.006
Mol.% End-members										
$CaThO_3$	0.00	0.00	0.48	0.00	0.00	0.07	0.12	0.49	0.22	0.07
$SrTiO_3$	0.42	0.31	0.44	0.58	2.07	2.70	6.58	9.27	7.36	5.19
$NaNbO_3$	0.00	0.00	0.00	0.00	4.02	1.83	6.55	0.51	1.08	1.74
$CaTiO_3$	97.51	97.69	96.86	94.48	89.45	86.85	79.96	36.41	58.21	78.92
Loparite	2.07	2.00	2.22	4.94	4.45	8.55	9.79	49.53	33.13	14.08
$Ce_2Ti_2O_7$	0.00	0.00	0.00	0.00	0.00	0.00	0.00	3.79	0.00	0.00

Compositions 1-8 Kapamba, Zambia: 1 & 2 P 1/5, 3 & 4 P 2/12, 5 P 10/2, 6 & 7 P 6/8; 8-10 Hills Pond, Kansas. Total Fe expressed as Fe_2O_3; n.d = not detected.

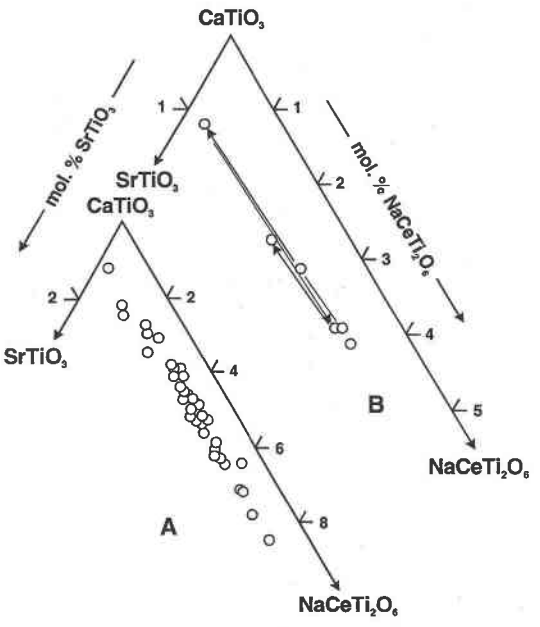

FIG. 5. Compositional variation (mol.%) of perovskite from the American Mine olivine lamproite. (A) Overall compositional range of discrete crystals; (B) typical core-to-rim patterns of zonation.

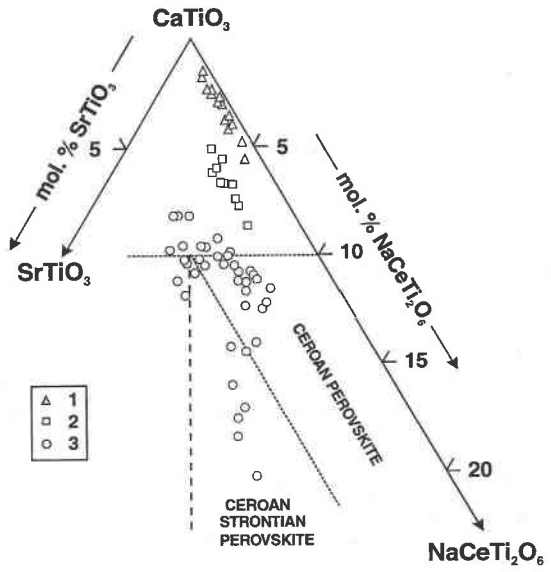

FIG. 6. Compositional variation (mol.%) of perovskite from the Kapamba olivine lamproites. Intrusions numbers (after Scott Smith *et al.* 1989): (1) P1/5, (2) P10/2, and (3) P6/8.

$(Si_{2.96}Al_{0.05})_{\Sigma 3.01}$ O_9] is an intermediate member of the solid-solution series between benitoite ($BaTiSi_3O_9$) and $K_2TiSi_3O_9$. The latter unnamed mineral, considered to be the Ti-analogue of wadeite, has been previously described from Middle Table Mountain lamproite (Leucite Hills) by Mitchell & Steele (1992).

BSE imagery shows the perovskite crystals to be very strongly zoned. Typically, three zones can be recognized: a petal- or star-shaped core, an intermediate zone and a rim (Fig. 2e). The petal-like pattern of zonation is due to the change in habit from cubic (core) to cubo-octahedral (intermediate zone plus rim), different growth rates of {100} and {111}, and different capacity of {100} and {111} to absorb the *LREE*. During crystallization, there was an increase in the growth rate of {100}, which apparently has higher *LREE*-absorbance capacity. Similar sectoral distribution of the *LREE* has been observed in tausonite from the Murun complex (Vorobyev *et al.* 1987), and in Sr-rich perovskite occurring in peralkaline nephelinite (Dawson *et al.* 1998). In contrast to the Hill Pond perovskite, tausonite crystals typically show some evidence of increasing growth-rate of the *LREE*-depleted octahedron faces from the core outward.

From the core toward the rim, the perovskite evolves by becoming enriched in Ca and Ti, and depleted in *LREE*, Na, K and Sr (Table 3, Fig. 7). The overall evolutionary trend is from K-rich (up to 1.5 wt.% K_2O) calcian strontian loparite to ceroan strontian perovskite at essentially constant Sr content. All three zones are unusual in containing significant amounts of Si (up to 1.9 wt.% SiO_2; verified by CAMECA SX–50 wavelength-dispersion electron microprobe). We are confident that the SiO_2 is a real constituent and not an artifact of the analysis due to excitation of the silicate matrix. Naturally occurring perovskite with *bona fide* high SiO_2 content has not been previously encountered.

Leucite Hills, Wyoming

Perovskite is found in only two varieties of lamproite from the Leucite Hills lamproite province (Mitchell & Bergman 1991). At Pilot Butte, perovskite occurs in an olivine-free madupitic diopside lamproite as euhedral to anhedral crystals in the groundmass ranging in size from 15 to 40 μm. The crystals are weakly zoned, but intergranular compositional variation is substantial, and the crystals range from perovskite *sensu stricto* to ceroan strontian perovskite (Table 4, Fig. 8). The perovskite at Pilot Butte is similar in composition to the most *REE*-, Sr-rich perovskite found at Kapamba.

In the Middle Table Mountain olivine-free transitional madupitic lamproite (Mitchell & Bergman 1991, Mitchell & Steele 1992), perovskite forms large (up to 180 μm) violet-colored oikocrysts enclosing leucite and diopside. Individual crystals exhibit no obvious zonation, but display significant intergranular ranges in composition, mainly in terms of their Ca, Na, Sr and *LREE* contents. Relative to perovskite from Pilot Butte, this perovskite is Sr and *REE*-rich (Table 4, Mitchell & Steele 1992), and compositions plot entirely within the field of ceroan–strontian perovskite (Fig. 8).

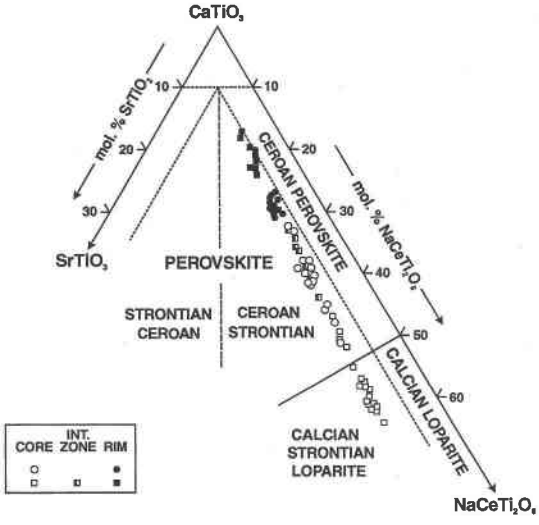

FIG. 7. Compositional variation (mol.%) of perovskite and loparite from the Hills Pond olivine lamproite.

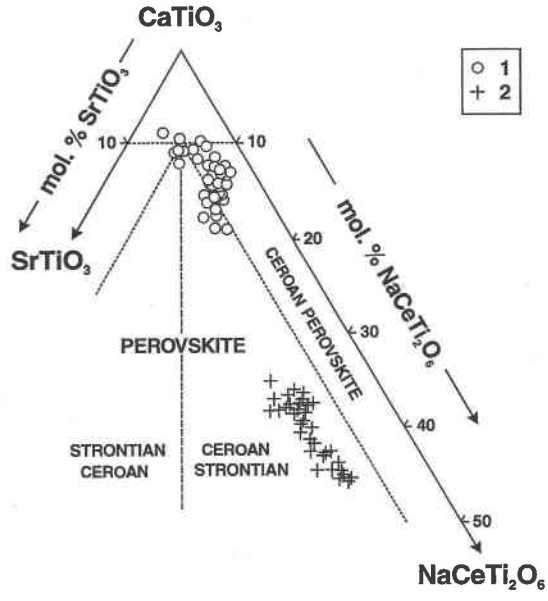

FIG. 8. Compositional variation (mol.%) of perovskite in madupitic lamproites from the Leucite Hills. (1) Pilot Butte; (2) Middle Table Mountain.

TABLE 4. REPRESENTATIVE COMPOSITIONS OF PEROVSKITE FROM TRANSITIONAL MADUPITIC LAMPROITES

Wt.%	1	2	3	4	5	6	7	8
Nb_2O_5	0.67	0.78	0.44	0.91	0.55	1.07	0.69	2.10
Ta_2O_5	0.45	0.92	0.24	0.90	0.34	0.38	0.12	0.53
TiO_2	54.70	53.90	55.06	54.21	50.06	49.31	49.49	49.96
Fe_2O_3	1.20	1.05	0.92	1.17	0.59	0.46	0.49	0.30
ThO_2	0.16	0.20	n.d	n.d	0.59	0.75	1.00	0.57
La_2O_3	1.66	0.16	1.43	1.18	3.66	2.41	4.48	3.04
Ce_2O_3	3.42	1.26	3.35	1.87	8.52	7.24	10.61	7.97
Pr_2O_3	n.d	0.35	n.d	n.d	1.18	2.16	1.56	0.78
Nd_2O_3	1.05	0.77	1.40	0.06	3.86	3.68	4.04	4.50
CaO	33.11	32.32	33.96	32.77	22.11	21.77	19.32	20.98
SrO	3.05	5.03	1.95	4.34	4.73	6.52	4.78	6.24
Na_2O	1.24	1.24	1.21	1.81	2.72	2.75	3.60	3.18
K_2O	0.20	0.17	n.d	n.d	0.30	0.26	0.35	0.50
Total	100.91	98.15	99.96	99.22	99.21	98.76	100.53	100.65
Structural formulae based on 3 atoms of oxygen								
Nb	0.007	0.009	0.005	0.010	0.006	0.013	0.008	0.024
Ta	0.003	0.006	0.002	0.006	0.002	0.003	0.001	0.004
Ti	0.974	0.980	0.981	0.974	0.976	0.968	0.972	0.965
Fe	0.021	0.019	0.016	0.021	0.012	0.009	0.010	0.006
Th	0.001	0.001	0.000	0.000	0.003	0.004	0.006	0.003
La	0.014	0.001	0.012	0.010	0.035	0.023	0.043	0.029
Ce	0.030	0.011	0.029	0.016	0.081	0.069	0.101	0.075
Pr	0.000	0.003	0.000	0.000	0.011	0.021	0.015	0.007
Nd	0.009	0.007	0.012	0.000	0.036	0.034	0.038	0.041
Ca	0.840	0.837	0.862	0.839	0.614	0.609	0.541	0.577
Sr	0.042	0.070	0.027	0.060	0.071	0.099	0.072	0.093
Na	0.057	0.058	0.056	0.084	0.137	0.139	0.182	0.158
K	0.006	0.005	0.000	0.000	0.010	0.009	0.012	0.016
Mol.% End-members								
$CaThO_3$	0.09	0.12	0.00	0.00	0.36	0.45	0.60	0.33
$SrTiO_3$	4.18	6.87	2.69	5.95	7.32	9.96	7.29	9.34
$NaNbO_3$	0.72	0.83	0.22	5.60	0.66	1.27	0.82	2.45
$CaTiO_3$	83.86	81.49	86.39	83.05	62.82	61.02	53.86	57.67
Loparite	11.15	10.69	10.70	5.40	28.84	27.30	37.43	30.21

Compositions 1-8 Leucite Hills, Wyoming: 1 & 2, 3 & 4 PB-1 and PB-3, respectively, Pilot Butte; 5 & 6, 7 & 8 MTM-5 and MTM-6, respectively, Middle Table Mt. Total Fe expressed as Fe_2O_3; n.d = not detected.

PEROVSKITE IN AGPAITIC NEPHELINE SYENITE PEGMATITES

In this work, we present new compositional data for Sr-rich loparite from two previously uninvestigated occurrences of agpaitic nepheline syenite pegmatite and compare these data with data previously published for Sr-bearing loparite found in agpaitic nepheline syenites from the Khibina and Lovozero complexes, Russia (Chakhmouradian & Mitchell 1998a, Mitchell & Chakhmouradian 1996, 1998, Kogarko *et al.* 1996).

Pegmatite Peak, Montana

In the agpaitic nepheline syenite pegmatites occurring at Pegmatite Peak (Rocky Boy stock, Montana; Pecora 1942), Sr-rich loparite (15–19 wt.% SrO) occurs as anhedral grains up to a few mm in size in association with alkali feldspar, aegirine, and lamprophyllite. Fractures in loparite are filled either with later-crystallizing crichtonite and niobian rutile or, more commonly, with silicates from the evolved agpaitic assemblage, together with Na–Nb-rich titanite and strontiochevkinite (Chakhmouradian & Mitchell 1998b).

The bulk of individual crystals are uniform in BSE images, although they commonly have a thin rim (6–20 μm) of material of high average atomic number. Table 5 and Figure 9 show that the uniform cores are strontian calcian loparite. The thin rim is composed of niobian loparite (Table 5, Fig. 9), with very low Sr and Ca contents (1.7–2.0 wt.% SrO and 0.8–1.0 wt.% CaO, respectively). Toward the rim, the Nb content increases from 1.7–5.1 to 17.7 wt.% Nb_2O_5 (Table 5), forming Nb-rich loparite belonging to the lueshite – loparite solid-solution series.

Gordon Butte, Montana

In agpaitic pegmatites occurring at Gordon Butte, Crazy Mountains, Montana (Dudás 1991), loparite forms euhedral to subhedral crystals associated with alkali feldspar, aegirine, eudialyte, barytolamprophyllite and Ba–Fe-bearing titanate of the hollandite group. The loparite shows a very limited compositional range (Table 5, Fig. 9) within and between crystals and is strontian calcian loparite with a relatively low Nb content (3.3–6.2 wt.% Nb_2O_5). Compared to loparite from Pegmatite Peak, it contains higher Ca and Th (2–3 wt.% CaO and ThO_2) and lower Sr (9.9–11.4 wt.% SrO).

Sr-bearing loparite from Pegmatite Peak and Gordon Butte is significantly enriched in Sr (10–19 wt.% SrO) and depleted in Nb (typically 3–6 wt.% Nb_2O_5), relative to loparite occurring in agpaitic syenites and pegmatites of the Khibina (1–3 wt.% SrO, 6–35 wt.% Nb_2O_5; Chakhmouradian & Mitchell 1998a) and Lovozero (1–7 wt.% SrO, 6–28 wt. % Nb_2O_5; Mitchell & Chakhmouradian 1996) complexes. Other minerals (titanite, chevkinite) at Pegmatite Peak are similarly rich in Sr, and these data suggest that the parental magmas of the Kola intrusions were relatively poor in Sr compared with those emplaced in the Wyoming craton.

Sr-BEARING ALKALINE ULTRAMAFIC ROCKS, KHIBINA, KOLA PENINSULA, RUSSIA

To complete our investigation of Sr-bearing perovskite compositional variation in the Khibina intrusion, we include in this study perovskite from the alkaline ultramafic suite (clinopyroxenite, olivine clinopyroxenite). In these rocks, which are not peralkaline, perovskite occurs as subhedral to anhedral crystals associated with titaniferous magnetite, clinopyroxene, olivine, phlogopite, apatite, pyrrhotite, ilmenite and, less commonly, with calzirtite and zirconolite. The mineral ranges in composition from perovskite *sensu stricto* to ceroan niobian perovskite (Table 5, Fig. 10). The latter is enriched in *LREE* (up to 18.1 wt.% $LREE_2O_3$), Na (up to 4.6 wt.% Na_2O), Nb (up to 6.7 wt.% Nb_2O_5) and Th (up to 3.7 wt.% ThO_2). The Sr content in perovskite may

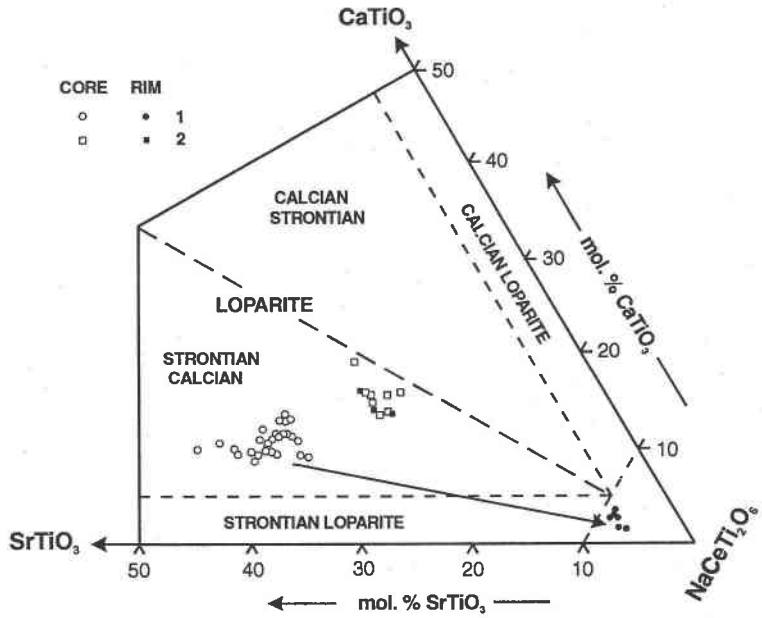

FIG. 9. Compositional variation (mol.%) of loparite from agpaitic nepheline syenite pegmatites. (1) Pegmatite Peak, Rocky Boy stock; (2) Gordon Butte.

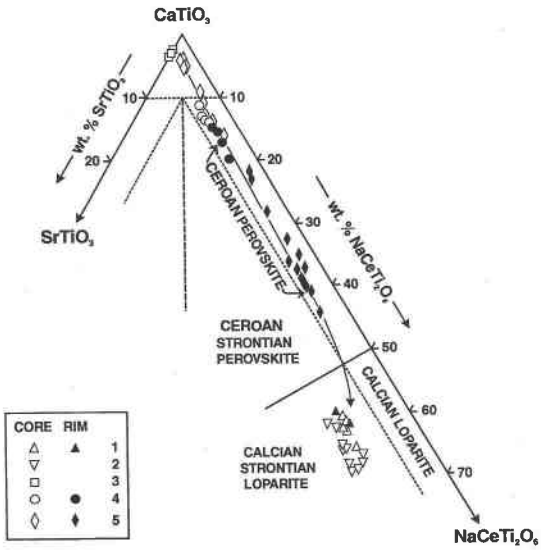

FIG. 10. Compositional variation (mol.%) of perovskite and loparite from alkaline ultramafic rocks of the Khibina complex. (1) ijolitized pyroxenite, Suduaiv; (2) ijolite, Eveslogchorr; (3) urtite, Patelichorr; (4) olivine clinopyroxenite, Olenii Ruchey; (5) olivine clinopyroxenite, Restinyun.

remain constant with increasing *LREE* and Na, or may slightly increase (# KHB–409: from 1.4 wt.% in the core to 2.4 wt.% SrO in the rim). Relatively Nb-poor (4.8–8.6 wt.% Nb_2O_5) calcian strontian loparite occurs in ijolites. The overall evolutionary trend is similar to the loparite trend established for the carbonatite complexes of the Kola Peninsula and the Schryburt Lake complex (Chakhmouradian & Mitchell 1997, Platt 1994). However, in contrast, the Sr contents (2.5–7 wt.% SrO) of perovskite and loparite from the Khibina ultramafic suite are significantly higher than in perovskite-group minerals from typical carbonatite complexes (<1 wt.% SrO).

These data show that perovskite from the ultramafic suite is richer in Sr than loparite in the more evolved agpaitic nepheline syenites of the Khibina complex. If the ultramafic suite represents a less evolved fraction of the magma that formed the Khibina intrusion, these data suggest that Sr contents of perovskite-group minerals decreased during differentiation. This conclusion contrasts with the behavior of Sr in perovskite-group minerals at Lovozero, where Sr has been found to increase during differentiation (Mitchell and Chakhmouradian 1996, Kogarko *et al.* 1996).

DISCUSSION AND CONCLUSIONS

The compositional variation of strontian perovskite and strontian loparite is summarized in Figure 11. From

TABLE 5. REPRESENTATIVE COMPOSITIONS OF PEROVSKITE AND LOPARITE FROM ALKALINE ULTRAMAFIC ROCKS AND PERALKALINE PEGMATITES

Wt.%	1	2	3	4	5	6	7	8	9	10	11	12
Nb_2O_5	0.08	6.16	6.14	3.26	n.d	8.00	5.79	4.04	3.82	3.47	5.14	17.70
Ta_2O_5	0.28	0.75	0.73	0.37	0.71	0.46	0.05	n.d	n.d	0.94	0.74	0.67
TiO_2	58.60	46.97	51.62	52.56	58.44	42.40	43.68	45.24	44.38	42.71	42.05	34.27
Fe_2O_3	0.10	0.79	0.53	0.42	0.43	0.41	1.27	0.33	0.60	0.11	0.26	0.20
ThO_2	0.28	0.70	0.57	n.d	0.10	2.16	1.05	3.07	2.65	0.85	1.74	2.20
La_2O_3	n.d	4.48	1.37	2.09	n.d	7.69	7.52	7.32	7.38	8.66	8.41	13.07
Ce_2O_3	0.56	8.42	2.85	5.01	n.d	13.02	14.65	14.95	14.38	13.35	14.28	18.38
Pr_2O_3	n.d	1.26	n.d	0.52	n.d	1.66	1.58	0.78	0.86	n.d	n.d	n.d
Nd_2O_3	0.32	3.60	0.48	1.03	n.d	2.05	2.84	3.11	2.68	2.99	3.15	2.79
CaO	38.77	21.00	30.38	29.64	38.91	10.83	10.78	5.28	5.00	2.87	3.30	0.76
SrO	1.54	2.36	2.52	2.50	1.91	5.18	6.15	9.87	11.40	18.85	16.55	1.67
Na_2O	0.61	4.12	2.68	2.41	0.94	6.12	5.72	6.08	5.72	5.39	5.92	9.99
Total	101.14	100.61	99.87	99.81	101.44	100.42	101.08	100.07	98.87	100.19	101.54	101.70
					Structural formulae based on 3 atoms of oxygen							
Nb	0.001	0.071	0.067	0.036	0.000	0.100	0.072	0.052	0.050	0.046	0.067	0.232
Ta	0.002	0.005	0.005	0.002	0.004	0.003	0.000	0.000	0.000	0.007	0.006	0.005
Ti	1.000	0.906	0.931	0.958	0.994	0.881	0.900	0.963	0.959	0.942	0.915	0.747
Fe	0.002	0.015	0.010	0.008	0.007	0.009	0.026	0.007	0.013	0.002	0.006	0.004
Th	0.001	0.004	0.003	0.000	0.001	0.014	0.006	0.020	0.017	0.006	0.011	0.015
La	0.000	0.042	0.012	0.019	0.000	0.078	0.076	0.076	0.078	0.094	0.090	0.140
Ce	0.005	0.079	0.025	0.044	0.000	0.132	0.147	0.155	0.151	0.143	0.151	0.195
Pr	0.000	0.012	0.000	0.005	0.000	0.017	0.016	0.008	0.009	0.000	0.000	0.000
Nd	0.003	0.033	0.004	0.009	0.000	0.020	0.028	0.031	0.028	0.031	0.033	0.029
Ca	0.943	0.577	0.780	0.770	0.943	0.321	0.317	0.160	0.154	0.090	0.102	0.024
Sr	0.020	0.035	0.035	0.035	0.025	0.083	0.098	0.162	0.190	0.321	0.278	0.028
Na	0.061	0.205	0.124	0.113	0.041	0.328	0.304	0.334	0.319	0.306	0.332	0.561
					Mol.% End-members							
$CaThO_3$	0.14	0.42	0.32	0.00	0.06	1.68	0.66	1.86	2.11	0.58	1.16	1.49
$SrTiO_3$	2.03	3.64	3.57	3.53	2.48	10.26	9.93	20.39	17.28	32.53	28.17	2.87
$NaNbO_3$	1.96	4.01	8.49	3.68	4.08	6.39	7.28	5.33	5.51	4.67	6.83	23.75
$CaTiO_3$	94.42	57.45	79.22	77.88	93.38	37.96	31.48	14.66	14.97	8.57	9.22	0.93
Loparite	1.45	34.48	8.40	15.41	0.00	41.63	47.16	57.76	60.13	52.85	53.74	67.46
$Ce_2Ti_2O_7$	0.00	0.00	0.00	0.00	0.00	2.08	3.49	0.00	0.00	0.80	0.88	3.50

Compositions 1-7 Khibina complex, Kola Peninsula, Russia: 1 & 2 olivine clinopyroxenite KHB-409, 3 & 4 olivine clinopyroxenite KHB-1752, 5 urtite KHB-1010, 6 ijolite KHB-1626, 7 ijolite KHB-72; 8 & 9 peralkaline pegmatite, Gordon Butte, Montana; 10-12 peralkaline pegmatite, Pegmatite Peak, Montana. Total Fe expressed as Fe_2O_3; n.d = not detected.

these data, and those presented by Mitchell (1995a, 1996), Mitchell & Vladykin (1993), Chakhmouradian & Mitchell (1998a) and Mitchell & Chakhmouradian (1996), it is apparent that:

1. Sr-bearing perovskite occurs in olivine lamproite, evolved orangeite, peralkaline nephelinite and ultramafic rocks associated with the Khibina alkaline complex.

2. Sr-bearing to Sr-rich loparite occurs primarily in agpaitic nepheline syenites and related rocks currently described as rheomorphic fenites (Haggerty & Mariano 1983, Mitchell 1996). Significant differences in the Sr content of loparite are found between intrusions.

3. Tausonite is very rare mineral encountered only in the ultrapotassic syenites of the Little Murun peralkaline complex.

4. Carbonatites and related ultramafic rocks associated with ijolite–carbonatite complexes (*e.g.*, Kovdor, Afrikanda, Oka, Magnet Cove) contain Sr-poor, Nb-rich perovskite-group minerals belonging to the perovskite – latrappite – lueshite – $Ca_2Nb_2O_7$ solid-solution series.

5. Kimberlites, alnöites and unevolved carbonate-bearing orangeites contain Sr-poor (<1 wt.% SrO) perovskite *sensu stricto*.

6. Perovskite-group minerals show extensive solid-solution between $SrTiO_3$ and $NaCeTi_2O_6$, but not between $SrTiO_3$ and $CaTiO_3$ (Fig. 11).

From these observations, we may conclude that Sr-rich perovskite and loparite are found in silicate rocks that lack primary carbonates, and Sr-poor perovskite forms in SiO_2-poor environments characterized by the presence of primary carbonate minerals and the absence of alkali feldspar and other tectosilicates. As the latter rocks may also contain Sr-, *REE*-rich fluorocarbonates [*e.g.*, the Benfontein calcite kimberlite (Mitchell 1994)], it would appear that the paucity of Sr-rich perovskite is not a simple consequence of a lack of Sr in their parental magmas. This conclusion is supported by preliminary experiments in the haplocarbonatite system $CaCO_3$–$Ca(OH)_2$–$SrTiO_3$ (Mitchell 1997), which indicate that in CO_2-bearing systems, Sr is preferentially partitioned into carbonates. Similar studies of tausonite–nepheline syenite systems have not yet been undertaken,

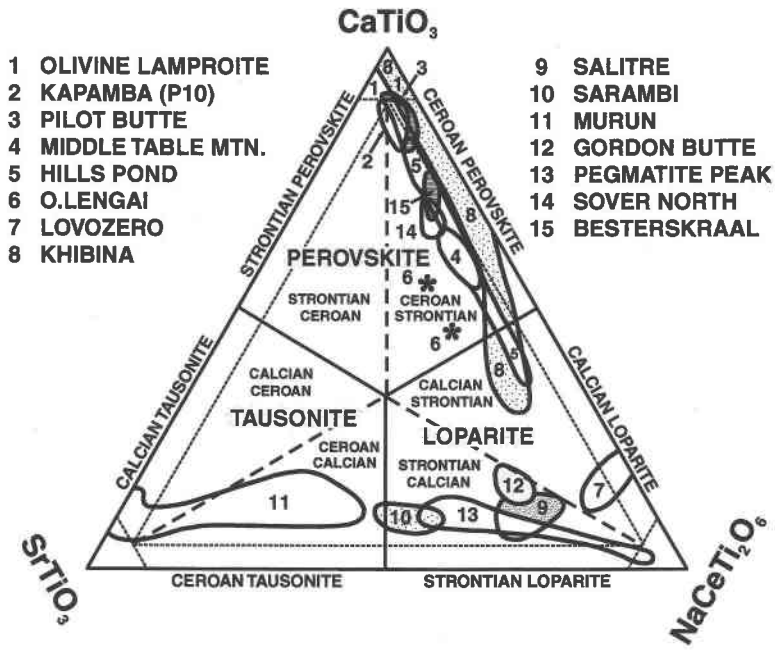

FIG. 11. Compositional variation (mol.%) of Sr-bearing perovskite, strontian loparite and ceroan calcian tausonite in the ternary system $CaTiO_3$ (perovskite) – $NaCeTi_2O_6$ [loparite-(Ce)] – $SrTiO_3$ (tausonite). 1, olivine lamproites, West Kimberley (Australia) and Arkansas (this work); 2, olivine lamproite P10, Kapamba, Zambia (this work); 3–4, madupitic lamproites from Pilot Butte and Middle Table Mountain, Leucite Hills, Wyoming (this work); 5, olivine lamproite, Hills Pond, Kansas (this work); 6, combeite nephelinite, Oldoinyo Lengai, Tanzania (Dawson & Hill 1998); 7 agpaitic nepheline syenites, Lovozero complex, Russia (Mitchell & Chakhmouradian 1996); 8, alkaline ultramafic rocks, Khibina complex, Russia (this work); 9–10, Salitre (Brazil) and Sarambi (Paraguay) rheomorphic fenites (Haggerty & Mariano 1983); 11, ultrapotassic syenite, Little Murun complex, Russia (Mitchell & Vladykin 1993); 12–13, Gordon Butte and Pegmatite Peak agpaitic nepheline syenite pegmatites, Montana (this work); 14–15, Sover North and Besterskraal orangeites, South Africa (Mitchell 1995). Note that perovskite in kimberlites and alnöites contains >90% mol.% perovskite *sensu stricto* (Mitchell 1995) and would plot in this figure close to the $CaTiO_3$ apex.

but are required to explain the apparent rarity of tausonite *sensu stricto* and how Sr is partitioned between titanates and silicates in agpaitic magmas.

The absence of naturally occurring perovskite belonging to the solid-solution series $CaTiO_3$ – $SrTiO_3$ is surprising given that complete solid-solution exists between these compounds in synthetic systems (Čeh *et al.* 1987). Their absence cannot as yet be explained, but must be related to the presence of other components in natural systems. The existence of a complete solid-solution series in natural perovskite-group minerals between tausonite and loparite is in agreement with experimental studies of the system $SrTiO_3$–$NaLaTi_2O_6$ (Mitchell & Chakhmouradian, unpubl. data; Farrell 1997).

There are no regular trends of compositional evolution evident in the population of perovskite and loparite investigated; thus Sr (and *REE*) may be enriched or depleted during crystallization. This observation suggests that there is no simple relationship between the Sr content of perovskite and the degree of differentiation of a particular rock in an alkaline complex or sequence. In the Leucite Hills lamproites, perovskite from Pilot Butte is less enriched in Sr and *REE* than perovskite from the more evolved Middle Table Mountain lamproite, in agreement with paragenetic and mineralogical data (Mitchell & Bergman 1991). However, a completely opposite trend of Sr- and *REE*-depletion is found in perovskite from the Hills Pond and American Mine lamproites.

The perovskite and loparite examined in this work are either of relatively uniform composition or show strong oscillatory zoning. Similar styles of complex

zonation are found in perovskite from olivine lamproite and tausonite–loparite from the Little Murun complex syenite (Mitchell & Vladykin 1993). This observation suggests that regardless of magma type, several stages of dissolution and growth are characteristic of the formation of individual crystals of perovskite. As coexisting minerals are not similarly zoned, it follows that such grains of perovskite may have crystallized as an early liquidus phase prior to emplacement of the magma that eventually formed their current host-rock; they certainly were not in equilibrium with that magma. Complex patterns of growth and resorption suggest crystallization in extremely fluid magmas that were undergoing turbulence and differentiation. On the other hand, weakly zoned or zonation-free perovskite and loparite, which form late-stage poikilitic plates in the groundmass, have undoubtedly crystallized *in situ*. The data presented above clearly demonstrate that perovskite-group minerals may form as early or late liquidus phases. No simple evolutionary trends of compositional variation with respect to Sr are evident. Speculation on petrogenetic aspects of the compositional variation and paragenesis we have documented is beyond the scope of this paper. In addition, we believe that such discussion is premature, as a variety of experimental studies involving perovskite-group minerals and diverse haplomagmas are required before any hypotheses can be advanced to explain our observations and conclusions.

Acknowledgements

This work is supported by the Natural Sciences and Engineering Research Council of Canada. Alan MacKenzie, Anne Hammond and Sam Spivak are thanked for technical assistance. John Lewis, Bob Cullers and Barbara Scott Smith are thanked for providing samples from West Kimberley, Hills Pond and Kapamba, respectively. Two anonymous referees are thanked for comments on an initial draft of this paper. Bob Martin is thanked for much editorial assistance.

References

Čeh, M., Kolar, D. & Golič, L. (1987): The phase diagram of $CaTiO_3$ – $SrTiO_3$. *J. Solid State Chem.* **68**, 68-72.

Chakhmouradian, A.R. & Mitchell, R.H. (1997): Compositional variation of perovskite-group minerals from carbonatite complexes of the Kola alkaline province, Russia. *Can. Mineral.* **35**, 1293- 1310.

_____ & _____ (1998a): Compositional variation of perovskite-group minerals from the Khibina complex, Kola Peninsula, Russia. *Can. Mineral.* **36**, 953-969.

_____ & _____ (1998b): Evolution of the accessory Sr–LREE and Ti–Nb mineralization in nepheline syenite at Pegmatite Peak, Montana. *Int. Mineral. Assoc., 17th Gen. Meeting (Toronto)*, A110 (abstr.).

Cullers, R.L., Ramakrishnan, S., Berendsen, P. & Griffin, T. (1985): Geochemistry and petrogenesis of lamproites, late Cretaceous age, Woodson County, Kansas, U.S.A. *Geochim. Cosmochim. Acta* **49**, 1383-1402.

Dawson, J.B. & Hill, P. (1998): Mineral chemistry of a peralkaline combeite–lamprophyllite nephelinite from Oldoinyo Lengai, Tanzania. *Mineral. Mag.* **62**, 179-196.

Dudás, F.Ö. (1991): Geochemistry of igneous rocks from the Crazy Mountains, Montana, and tectonic models for the Montana alkalic province. *J. Geophys. Res.* **96**, 13261-13277.

Edgar, A.D. & Mitchell, R.H. (1997): Ultrahigh pressure–temperature melting experiments on an SiO_2-rich lamproite from Smoky Butte, Montana: derivation of siliceous lamproite magmas from enriched sources deep in the continental mantle. *J. Petrol.* **38**, 457-477.

Farrell, S. (1997): *Crystallographic Studies of Selected Perovskite-Group Compounds*. M.Sc. thesis, Lakehead Univ., Thunder Bay, Ontario.

Haggerty, S.E. & Mariano, A.N. (1983): Strontian-loparite and strontiochevkinite: two new minerals in rheomorphic fenites from the Parana Basin carbonatites, South America. *Contrib. Mineral. Petrol.* **84**, 365-381.

Jaques, A.L., Lewis, J.D. & Smith, C.B. (1986): The kimberlites and lamproites of Western Australia. *Geol. Surv. Western Australia, Bull.* **132**.

Kogarko, L.N., Williams, C.T. & Osokin, E.D. (1996): Compositional evolution of loparite from the Lovozero massif. *Geokhimiya*, 294-297 (in Russ.).

Mason, B. (1977): Elemental distribution in minerals from the Wolgidee Hills intrusion, Western Australia. *New Zealand D.S.I.R. Bull.* **218**, 114-120.

Mitchell, R.H. (1994): Accessory rare earth, strontium, barium and zirconium minerals from the Benfontein and Wesselton calcite kimberlites, South Africa. *In* Proc. Fifth Int. Kimberlite Conf. **1** (H.O.A. Meyer & O.H. Leonardos, eds.). *Companhia de Pesquisa de Recursos Minerais (Brasilia), Spec. Publ.* **1A**, 115-128.

_____ (1995a): *Kimberlites, Orangeites and Related Rocks*. Plenum Publ. Corp., New York, N.Y.

_____ (1995b): Melting experiments on a sanidine phlogopite lamproite at 4–7 GPa and their bearing on the sources of lamproitic magmas. *J. Petrol.* **36**, 1455-1474.

_____ (1996): Perovskites: a revised classification scheme for an important rare earth element host in alkaline rocks. *In* Rare Earth Minerals: Chemistry, Origin and Ore Deposits (A.P. Jones, F. Wall & C.T. Williams, eds.). *Mineral. Soc Ser.* **7**. Chapman & Hall, London, U.K. (41-76).

_____ (1997): Preliminary studies of the solubility and stability of perovskite group compounds in the synthetic carbonatite system calcite–portlandite. *J. Afr. Earth Sci.* **25**, 147-158.

_____ & BERGMAN, S.C. (1991): *Petrology of Lamproites.* Plenum Publ. Corp., New York, N.Y.

_____ & CHAKHMOURADIAN, A.R. (1996): Compositional variation of loparite from the Lovozero alkaline complex, Russia. *Can. Mineral.* **34**, 977-990.

_____ & _____ (1998): Th-rich loparite from the Khibina complex, Kola Peninsula: isomorphism and paragenesis. *Mineral. Mag.* **62**, 341-353.

_____ & REED, S.J.B. (1988): Ion microprobe determination of rare earth elements in perovskite from kimberlites and alnöites. *Mineral. Mag.* **52**, 331-339.

_____ & STEELE, I. (1992): Potassian zirconium and titanium silicates and strontian cerian perovskite in lamproites from the Leucite Hills, Wyoming. *Can. Mineral.* **30**, 1153-1159.

_____ & VLADYKIN, N.V. (1993): Rare earth element-bearing tausonite and potassium barium titanates from the Little Murun potassic alkaline complex, Yakutia, Russia. *Mineral. Mag.* **57**, 651- 664.

PECORA, W.T. (1942): Nepheline syenite pegmatites, Rocky Boy Stock, Bearpaw Mountains, Montana. *Am. Mineral.* **27**, 397- 424.

PLATT, R.G. (1994): Perovskite, loparite and Ba–Fe hollandite from the Schryburt lake carbonatite complex, northwestern Ontario, Canada. *Mineral. Mag.* **58**, 49-57.

SCOTT SMITH, B.H., SKINNER, E.M.W. & LONEY, P.E. (1989): The Kapamba lamproites of the Luangwa valley, eastern Zambia. *In* Kimberlites and Related Rocks. Proc. Fourth Int. Kimberlite Conf. **1** (J. Ross, A.L. Jaques, J. Ferguson, D.H. Green, S.Y. O'Reilly, R.V. Danchin & A.J.A. Janse, eds.). *Geol. Soc. Aust., Spec. Publ.* **14**, 189-205.

VOROBYEV, E.I., KONYEV, A.A., MAYSHONOK, Y.V., AFONINA, G.G. & PARADINA, L.F. (1987): *Tausonite: Geological Conditions of Formation and Mineral Paragenesis.* Nauka Press, Novosibirsk, Russia (in Russ.).

_____, _____, _____, _____ & SAPOZHNIKOV, A.N. (1984): Tausonite, $SrTiO_3$, a new mineral of the perovskite group. *Zap. Vses. Mineral. Obshchest.* **113**(1), 86-89 (in Russ.).

Received July 13, 1998, revised manuscript accepted February 28, 1999.